Downloaded from orbit.dtu.dk on: May 04, 2023

DTU Library

The effects of mixing air distribution and heat load arrangement on the performance of ceiling radiant panels under cooling mode of operation

Mustakallio, Panu ; Kosonen, Risto ; Melikov, Arsen Krikor

Published in:
Science and Technology for the Built Environment

Link to article, DOI:
10.1080/23744731.2016.1262662

Publication date:
2016

Document Version
Peer reviewed version

Link back to DTU Orbit

Citation (APA):
Mustakallio, P., Kosonen, R., & Melikov, A. K. (2016). The effects of mixing air distribution and heat load arrangement on the performance of ceiling radiant panels under cooling mode of operation. *Science and Technology for the Built Environment*, *23*(7), 1090-1104. https://doi.org/10.1080/23744731.2016.1262662

General rights
Copyright and moral rights for the publications made accessible in the public portal are retained by the authors and/or other copyright owners and it is a condition of accessing publications that users recognise and abide by the legal requirements associated with these rights.

- Users may download and print one copy of any publication from the public portal for the purpose of private study or research.
- You may not further distribute the material or use it for any profit-making activity or commercial gain
- You may freely distribute the URL identifying the publication in the public portal

If you believe that this document breaches copyright please contact us providing details, and we will remove access to the work immediately and investigate your claim.

ACCEPTED MANUSCRIPT

The effects of mixing air distribution and heat load arrangement on the performance of ceiling radiant panels under cooling mode of operation

PANU MUSTAKALLIO[1,*], RISTO KOSONEN[2], and ARSEN MELIKOV[3]

[1]*Halton Oy, Haltonintie 1-3, 47400 Kausala, Finland*

[2]*Department of Mechanical Engineering, Aalto University, Sähkömiehentie 4, 02150 Espoo, Finland*

[3]*International Centre for Indoor Environment and Energy, DTU Civil Engineering, Technical University of Denmark, Nils Koppels Alle, Building 402, 2800 Lyngby, Denmark*

Received 14 Aug 2016; accepted 11 Nov 2016

Panu Mustakallio, MSc, is a Development Manager and a PhD Student. **Risto Kosonen, PhD,** Member ASHRAE, is a Professor. **Arsen Melikov, PhD,** Fellow ASHRAE, is a Professor.

*Corresponding author e-mail: panu.mustakallio@halton.com

The cooling power of radiant panels can be effected by the arrangement of heat loads and by the room air distribution system. This impact can be important because often the cooling output is the critical factor for the design and usability of radiant panels. In this study, the impact of heat load arrangement and air distribution generated in a room by linear slot diffuser, radial multi-nozzle diffuser and radial swirl induction unit on the cooling power of radiant panels was compared. The impact on the thermal environment was also studied. Measurements were carried out without and with supply air in a test chamber equipped with two ceiling radiant panels and

ACCEPTED MANUSCRIPT

ACCEPTED MANUSCRIPT

air distribution units flush with the radiant panels. Heat load was generated through the walls and with heated cylinders. The cooling power of the radiant panels was increased with the studied air distribution methods. The increase was from 5% to 17% depending on the air distribution method and the heat load arrangement. The most significant effect of the heat load arrangement occured when heat loads are located unevenly and their convection flow turns or weakens the supply air jet flushing the radiant panels.

ACCEPTED MANUSCRIPT

ACCEPTED MANUSCRIPT

Introduction

The objective of this study was to identify the impact of mixing air distribution generated in a room by ceiling installed linear slot diffuser, radial multi-nozzle diffuser and radial swirl induction unit on the cooling power of ceiling radiant panel (CRP). The importance of heat load distribution in the room on the cooling power of CRPs was studied. The impact of the generated air distribution and heat load arrangement on the thermal environment in the room was also studied.

The average share of the existing building stock is as high as 40% of the overall energy usage in the EU member countries (Kurnitski et al. 2013). To reduce the energy use of new buildings, Energy Performance of Buildings Directive (EPBD) requires that all new buildings in the European Union must be nearly zero energy buildings (nZEB) from 31st December, 2020 and public owned buildings must be nearly zero energy building from 31st December, 2018 (European Commission EPBD recast 2010). According to the European Commission, improved energy efficiency of buildings means maintaining good indoor air quality and thermal comfort level with less energy use than before (European Commission: Energy Efficiency in the European Union). CRP systems have been studied actively. The research data and design guidelines of radiant systems (Babiak et al. 2007) and mixing ventilation (Müller et al. 2013) have been summarized in the guidebooks by Federation of European Heating, Ventilation and Air Conditioning Associations (REHVA). The research on radiant cooling and heating systems during the last 50 years has been reviewed (Rhee et al. 2015). CRPs have been seen as one

ACCEPTED MANUSCRIPT

ACCEPTED MANUSCRIPT

potential solution for future nZEB that simultaneously provides excellent indoor climate and energy efficient opeation over traditional all-air systems in office buildings.

The research of cooling capacity of CRPs has been reported in numerous publications. The main research question has been the radiant and convective heat transfer mechanism from cooled CRP surface. Several full-scale tests of cooling performance of different CRPs with cooling water circulation have been reported (Ardehali et al. 2003, Jeong et al. 2003, 2004 and 2006, Novoselac et al. 2006, Causone et al. 2009, Diaz et al. 2009 and 2010, Fonseca et al. 2010 and 2011, Andrés-Chicote et al. 2012, Tian et al. 2012, Zhang et al. 2013, Niu et al. 2014, Yuan et al. 2015). Most studies have been done with solid or perforated CRP with acoustic mat, preventing air flow through CRPs. The CRPs can be in flush installation within the false ceiling or in exposed installation. Top insulation of CRP is used to prevent the excess cooling of the space above the suspended ceiling (Jeong et al. 2004) whereas in exposed installation top surface without insulation increases the cooling power of CRP (Jeong et al. 2006). The flush installation was carried out also in some earlier research with CRPs constructed with capillary tube mats and embedded into the plaster (Diaz et al. 2009 and 2010, Fonseca et al. 2010, Yuan et al. 2015). CRPs with openings allowing the room air to flow through and to increase their convective cooling power (can be considered as hybrid CRP – passive chilled beam solution) have been studied as well (Tian et al. 2012, Zhang et al. 2013, Niu et al. 2014). The cooling power of CRP can be affected by the room air distribution system. This impact can be an important because often the cooling output is the critical factor for the design and usability of CRPs. The cooling power of CRPs may also be effected by the arrangement of heat loads in the room because the

ACCEPTED MANUSCRIPT

ACCEPTED MANUSCRIPT

operation of the panels is based on the combination of free convection and radiation heat transfer. Without air distribution and with uniform heat load distribution an average portion of radiation 56% and convection 44% is reported in earlier research (Causone et al. 2009, Andrés-Chicote et al. 2012).

In most publications, total cooling capacity of CRPs was measured in full-scale test setup from supply and return water temperatures and water mass flow rate. Then total (sum of radiant and convective) heat transfer coefficient is calculated by dividing the cooling capacity with the measured temperature difference of the CRP surface temperature and room (reference) temperature. After that portion of radiant heat transfer has been calculated when knowing the room dimensions, view factors (calculated), emissivity and temperatures (measured) of surrounding surfaces as well as difference between CRP surface temperature and room air temperature. The convective heat transfer coefficient is obtained by subtracting radiant heat transfer coefficient from the total heat transfer coefficient. In the earlier research, it was stated that radiant heat transfer coefficients from cooled CRP surface in measured test setups were nearly constant at typical cooling water and room temperature (Causone et al. 2009, Andrés-Chicote et al. 2012, Zhang et al. 2013). The influence of radiant proportion of heat source (radiant proportion of radiant and convective heat transfer) on the cooling capacity of CRP system was reported in the earlier research by using computational model and laboratory measurements (Niu et al. 2014). It stated that the radiant heat transfer coefficient of CRP surface can differ depending on the radiant proportion of the heat source. According to that, the cooling capacity of CRP system should be defined with internal heat sources due to the larger convective

ACCEPTED MANUSCRIPT

ACCEPTED MANUSCRIPT

proportion of heat sources and a slightly smaller total capacity of CRP system (about 12 %). The ceiling coverage ratio of CRP (portion of the ceiling area covered by CRP) affects also the cooling capacity of CRP system, higher cooling capacity was obtained at lower ceiling coverage ratio of CRPs (Jeong et al. 2007). There was discussed that this capacity enhancement maybe comes from increased free air movement around the CRPs and increased radiation heat flux per unit CRP area with decreased ceiling coverage ratio. According to that, the ceiling coverage ratio effects on the CRP heat transfer are not clearly known. For instance different room shapes (room lenght/width aspect ratios 1:1, 2:1 or 3:2) didn't hardly effect the radiant heat transfer coefficient in the cases with uniform heat source distribution, except in the case with non-uniform heat sources when the radiant heat transfer changes significantly (Niu et al. 2014). Typical effect of ceiling coverage area for the cooling power of the flush installation of CRPs with or without insulation on top is presented in EN-14240 (2004) standard. The biggest impact to the cooling performance of CRPs was reached with supply air distribution over the panel surface due to the change of the mode of convection from natural to forced convection, or mixed convection (Jeong et al. 2003, Fonseca et al. 2010, Tian et al. 2012).

The effect of mixing air distribution on the cooling performance of CRPs was studied earlier with top insulated metal CRPs in a test room with full radiant ceiling (Jeong et al. 2003, 2004). Multi-nozzle supply air diffuser installed in the wall near the ceiling was used with supply air at the same temperature as room temperature directed along whole ceiling surface with inlet velocity of the diffuser 2, 4 and 6 m/s (6.56, 13.12 and 19.69 ft/s). It was concluded that the cooling power of the CRP system can be increased by approximately 12, 23 and 35%. The use of

ACCEPTED MANUSCRIPT

ACCEPTED MANUSCRIPT

only supply air at the same temperature as room temperature in that research does not represent well the situation in typical modern office building with high temperature cooling system like CRPs. In high temperature cooling systems, supply air is almost always cooled to approximately 12 - 14 °C (53.6 - 57.2 °F) in the central air handling unit and supplied into the room in 16 °C (60.8 °F) in the middle European climate. This is required for maintaining room air dew point in a low enough temperature and air humidity level as recommended in design criteria (Woollett et al. 2015). Supply air temperature can be a bit higher with desiccant cooling system. When 16 °C (60.8 °F) air is supplied over the CRP, convective heat transfer coefficient is enhanced due to the forced or mixed convection, but the temperature of entrained supply air on the surface of the CRP is lower reducing the convective heat transfer. The effect of mixing air distribution was also studied in the same research setup with CRP in exposed installation (Jeong et al. 2007). Earlier research of the effect of mixing ventilation on the cooling performance of CRPs has been reported also in the test setup with a high aspiration supply air diffuser (consisting of row of supply air nozzles) installed between two CRPs in flush installation within the false ceiling (Novoselac et al. 2006). The supply air jets in that test setup were not flushing the surfaces of CRPs, but supplied with very high velocity onto the ceiling surface between CRP and the entrainment air increased the convection heat transfer from CRPs. The conculsion was that convection heat transfer was increased by 4 – 17%. In the study, supply air at the same temperature as room temperature was used based on the assumption that high entrainment of room air changed the supply air jet temperature fast to nearly the same temperature as room temperature. The initial velocity in the supply air nozzles was 15 m/s (49.21 ft/s), which was a very high initial velocity requiring very high ductwork pressure and generating high sound level.

ACCEPTED MANUSCRIPT

ACCEPTED MANUSCRIPT

In another research, a full-scale test setup representing two office rooms in a real office building with top-insulated CRP system in flush installation and supply air distribution from small radial diffusers (Diaz et al. 2010) was build. The effect of supply air distribution was measured in typical operating conditions in cooling conditions with 16 °C (60.8 °F) supply temperature. The effect to the cooling performance of CRPs was 6%. The compensating heat loads were generated with heated window surface on one wall and with heat dummies distributed near the window wall. The effect of mixing ventilation on the heating performance of CRPs was also measured in that research. This was reported to be much larger, about 30%, which was logical, because in heating conditions there is nearly no natural convection from CRPs.

The effect of heat load arrangement on the cooling performance of CRPs was studied earlier with hybrid metal CRPs allowing the room air to flow through in an exposed installation. The compensating heat load was conducted in three cases: in the first case through all four walls and floor of the test room, in the second case only through one wall and in the third case generated with four symmetrically located internal dummy heat loads (Niu et al. 2014). It was concluded that the compensating heat load conducted through all walls and floor increased the cooling capacity of hybrid CRPs by 13%, and only through one wall increased by 10% when comparing with the case with internal dummy heat loads. Different proportion of the radiant heat transfer of heat sources effected the proportion of radiant heat transfer of CRPs. According to that, with internal heat sources (heated cylinders similar as those used in the present study) radiant proportion was 0.615 and with external heat sources uniformly on all wall and floor surfaces 0.66 with a difference of 10 ^{0}C (18 °F) between room and mean water temperatures.

ACCEPTED MANUSCRIPT

ACCEPTED MANUSCRIPT

In the present study, generic, solid ceiling integrated CRP system was studied. The effect of air distribution was studied with typical supply air temperature and with operating data used in modern office environment with a high temperature cooling system. The effect of air distribution was studied with different supply air diffuser types based on the different jet types and also characteristics of supply air jets were calculated. Also the effect on cooling performance of novel swirl induction unit was studied. The simultaneous effect of both air distribution and heat load arrangement has not been studied in any of the earlier reported researches, which justified the present study.

Methods

A full-scale test room 4.7 m (15.42 ft) (L), 3.0 m (9.84 ft) (W) and 2.5 m/ 2.8 m (8.20 ft/ 9.19 ft) (false ceiling H/ H) was equipped with two top insulated CRPs with dimensions 3 m (9.84 ft) x 0.6 m (1.97 ft). The panels were installed near to the long walls of the room. The air distribution units, linear slot diffuser, radial multi-nozzle diffuser and radial swirl induction unit, where installed in the middle of the false ceiling so that the supply air jet was flushing the CRPs. The test room was constructed according EN-15116/EN-14518 (2008) standard to allow for accurate measurement of the cooling power of the chilled beams and also following guidelines detailed in the chilled ceiling testing standard EN-14240 (2004). The construction of the full-scale test room is presented in Fig. 1. All surfaces of the test room were built with 8 mm (0.315 in) thick plywood on timber battens. The external room where the test room was built was well insulated from the ambient environment. Air circulation fans were used for maintaining constant

ACCEPTED MANUSCRIPT

ACCEPTED MANUSCRIPT

air temperature in the external room surrounding the test room. External room air was also in contact with the test room floor construction along five 75 mm (2.95 in) high and 550 mm (21.65 in) wide lengthwise air passages. There was 25mm (0.984 in) thick particle board on top of the air passages and at the timber battens, and as the test room floor covering, 8mm (0.315 in) thick plywood. The surfaces of the test room were sealed for minimizing the infiltration of air between the test room and the external room.

Tests were performed without supply air and with the three air distribution methods (linear slot diffuser, radial multi-nozzle diffuser and radial swirl induction unit). All cases with air distribution were done with 25 l/s (1.8 l/s/m^2_{floor}) (52.97 cfm [0.3543 cfm/ft^2_{floor}]) and 16 ^{0}C (60.8 °F) supply air. For reaching 26 ^{0}C (78.8 ^{0}F) test room air temperature at 1.3 m (4.27 ft) height from the floor, a compensating heat load was conducted either through test room walls and floor by adjusting the external room temperature warmer than the test room temperature or by eight heated dummies with adjustable electrical power supply. The supply air flow rate and room temperature represented typical indoor climate design criteria for two person office room with low polluting building emissions according EN 15251 (2007) standard. The heat load division differed from the real office room cases, but provided guidelines for real applications.

Inlet water temperature for the radiant panels was 15 ^{0}C (59.0 ^{0}F) and water flow rate was adjusted to 0.043 kg/s (0.0948 lb/s), which led to an outlet water temperature 17 ^{0}C (62.6 ^{0}F) in the case without supply air. These were typical operating parameters in real office buildings. With the cases where air distribution was introduced, outlet water temperature varied. Relative

ACCEPTED MANUSCRIPT

ACCEPTED MANUSCRIPT

humidity in the test room varied between 10% - 30% during measurements with maximum 7 ^{0}C (44.6 ^{0}F) dew point temperature, which prevented the risk of condensation. Cooling power of ventilation air supplied at 16 ºC (60.8 ^{0}F) was approx. 22 W/m$^2_{floor}$ (6.97 Btu/h/ft$^2_{floor}$) and of the CRPs 28 W/m$^2_{floor}$ (8.88 Btu/h/ft$^2_{floor}$). Cooling power of the CRPs was calculated from the water temperature difference and mass flow rate. Conductance of CRPs were calculated by dividing the cooling power with the temperature difference of the mean water temperature and average room air temperature at 1.3 m (4.27 ft) height (from four locations measured). Exponent n = 1.083 for the temperature difference was based on CRP's manufacturer data. Equation (1) for conductance is shown below (Zehnder Carboline 2010).

$$Conductance = \frac{q_{m,water} \cdot c_{p,water} \cdot (T_{water\ out} - T_{water\ in})}{\left(T_{room} - \frac{T_{water\ out} + T_{water\ in}}{2}\right)^n} \quad (1)$$

Conductance = Conductance of CRPs, W/K (Btu/h/°F)

$q_{m,water}$ = Water mass flow rate, kg/s (lb/h)

$c_{p,water}$ = Water heat capacity, kJ/kg/K (Btu/lb/°F)

T = Temperature of water in to radiant panel, water out or room air, K (°F)

The water flow rate was measured with electromagnetic flowmeter and air flow rate with orifice plate flowmeter. Temperatures were measured with PT-100 temperature sensors. The measurement systems are designed for maintaining very stable conditions and are calibrated regularly for maintaining tolerances required by the EN standard. The accuracy requirement for water flow rate is +/- 0.5 % and for air flow rate is +/- 3 %. Accuracy requirement for water

ACCEPTED MANUSCRIPT

ACCEPTED MANUSCRIPT

temperature +/- 0.7 % (+/- 0.1 ^{0}C [0.18 ^{0}F]) and for water temperature difference is +/- 0.9 % (+/- 0.2 ^{0}C [0.36 ^{0}F]). Accuracy requirement for air temperature is +/- 0.8 % (+/- 0.2 ^{0}C [0.36 ^{0}F]), and for temperature difference between reference room temperature and mean water temperature +/- 1.2 % (+/- 0.1 ^{0}C [0.18 ^{0}F]). Accuracy of the test setting with heat loads according to the standard is estimated to +/- 3 %. The total accuracy of the cooling power measurement of the radiant panels is +/- 2.7 %. This is calculated from the accuracy of the parameters in the equation (1), from the accuracy of the test setting and from the accuracy of the air flow measurement by using the cumulative error law. The accuracy of the air flow measurement is estimated to +/- 1.5 % due to its indirect effect to the cooling power.

Room air temperature (T) was measured at four locations and vertical temperature difference at one location. Air temperature sensors were shielded from radiation. Black ball temperature (Tbb) was measured at two locations. Supply air flow pattern was visualized with smoke. The top view of the full-scale test room and the temperature measurement locations and heights are shown in Fig. 2.

Effect of air distribution

The effect of air distribution was tested in the four different mixing ventilation arrangements: two lengths of linear slot diffuser, radial multi-nozzle diffuser (with 4 x 4 adjustable nozzles) and radial swirl induction unit with/ without additional cooling of induction air in the coil of the induction unit. Linear slot diffusers were 3 m (9.84 ft) long with 2 mm (0.0787 in) slot height in the case 2 and 0.9 m (2.95 ft) long with about 10 mm (0.394 in) slot height in the case 2B. The

ACCEPTED MANUSCRIPT

ACCEPTED MANUSCRIPT

induction ratio (volume flow of air jet leaving the unit / supply air flow from nozzles) of swirl induction unit was 2.8 at studied operating point according to the manufacturer's product data. The centerline velocity, volume flow rate and average temperature of the supply air jet from studied diffuser types at the location just before the CRP surface was evaluated with manufacturer calculation tool (Halton HIT Design 20015). It was based on semi-empirical turbulent air jet equations (Hagström et al. 1999) of Grimitlyn (2) and (3) for linear jet and (4) and (5) for radial jet. Throw length coefficients K_1 for attached linear and radial jets and supply air jet initial opening height / area for equations were based on manufacturer's product data. The average temperature of the supply air jet was calculated with equation (6).

$$v_X = v_0 \cdot K_1 \cdot \sqrt{\frac{H_0}{X}} \quad (2)$$

$$Q_X = Q_0 \cdot \frac{\sqrt{2}}{K_1} \cdot \sqrt{\frac{X}{H_0}} \quad (3)$$

$$v_X = v_0 \cdot K_1 \cdot \frac{\sqrt{A_0}}{X} \quad (4)$$

$$Q_X = Q_0 \cdot \frac{\sqrt{2}}{K_1} \cdot \frac{X}{\sqrt{A_0}} \quad (5)$$

ACCEPTED MANUSCRIPT

ACCEPTED MANUSCRIPT

$$t_X = \frac{t_0 \cdot Q_0 + t_{room} \cdot (Q_X - Q_0)}{Q_X} \quad (6)$$

v_X = Centerline velocity of supply air jet at distance X, m/s (ft/s)

v_0 = Supply air jet initial opening velocity, m/s (ft/s)

K_1 = Supply air jet throw length coefficient, -

H_0 = Height of linear jet, m (ft)

X = Distance of supply air jet from opening, m (ft)

Q_X = Volume flow rate of supply air jet at distance X, l/s (cfm)

Q_0 = Initial volume flow rate of supply air jet, l/s (cfm)

A_0 = Radial jet initial opening area, m^2 (ft^2)

t_0 = Supply air jet initial temperature, °C (°F)

t_X = Supply air jet average temperature at distance X, °C (°F)

The test cases are shown in Fig. 3 and photos of the test setup with smoke visualizations of the supply air jet in Fig. 4. Smoke visualizations were used to ensure that supply air jets were fully flushing the CRPs. The shortest distance between CRPs and supply air diffuser was 0.85 m (2.79 ft) with the linear diffuser, 0.77 m (2.53 ft) with the multi-nozzle diffuser and 0.63 m (2.07 ft) with the swirl induction unit.

ACCEPTED MANUSCRIPT

ACCEPTED MANUSCRIPT

Measured case parameters and cooling powers are shown in Table 1. The compensating heat load was conducted through the test room walls and floor in all cases. The additional cooling power of induction unit's coil in the last case (5) was 17 W/m^2_{floor} (5.39 $Btu/h/ft^2_{floor}$).

Effect of heat load arrangement

The effect of heat load arrangement was studied with and without air distribution. The radial multi-nozzle diffuser in the test cases was used with air distribution. The test cases are shown in Fig. 5 and listed in Table 2 with measured case parameters and cooling powers. Photos of smoke visualizations of test set-ups are shown in Fig. 6. Smoke was used for visualizing the supply air jet flushing the CRPs with different heat load arrangements. In case 1, compensating heat loads were conducted through the walls of test room. In case 1B, the compensated heat loads were located symmetrically inside the test room. Ambient temperature at the same temperature as room temperature was used by adjusting the external temperature to the same as the average room temperature at 1.3 m (4.27 ft) height. Supply water temperature and mass flow rate were kept same as in the case 1. Cases 3, 3B and 3C were done similar way as cases 1 and 1B, but with supply air. In the last case, the effect of uneven heat load arrangement was measured (Fig. 5, Case 3C).

The case 1B was done mostly according to the chilled ceiling testing standard EN-14240 (2004). The test room fulfilled the accuracy criteria and heated dummies according to the chilled ceiling testing standard were used. The structure of the heated dummy was consisted of 1.0 m (3.28 ft) long cylinder of painted sheet metal with diameter of 0.3 m (0.984 ft). Distance to the

ACCEPTED MANUSCRIPT

ACCEPTED MANUSCRIPT

bottom cover plate from floor was 0.05 m (0.164 ft) and to the cylinder 0.1 m (0.328 ft) from floor. Top of the cylinder was closed with cover plate. Room air was circulated freely from 0.05 m (0.164 ft) opening between the bottom cover plate and bottom of the cylinder, and through four holes of diameter 0.1 m (0.328 ft) in the upper side of the cylinder. Heating element in the cylinder was consisted of three adjustable 60 W (205 Btu/h) lamps in the middle with 0.2 m (0.656 ft), 0.4 m (1.31 ft) and 0.6 m (1.97 ft) heights from floor. There were some differences to the chilled ceiling testing standard: the heated dummies were located correctly, but there were 8 dummies instead of 10 dummies, and 26% of the ceiling was covered with CRPs, but not at least 70% as suggested in the standard. The electric power of 376 W (1283 Btu/h) of the heated dummies in the case 1B was defined according to the product data of CRPs in the targeted operating conditions. In the case 3B and 3C, the electric power was increased with 296 W (1010 Btu/h) according to the cooling power of the supply air flow.

Surface temperatures and electric power of heated dummies in different cases are listed in Table 3. Wall temperatures were measured with PT-100 temperature sensors (accuracy +/- 0.2 ^{0}C [0.36 ^{0}F]) from one location in the middle of wall surface and floor surface temperature from one location near the 4.7 m (15.42 ft) long wall. Surface temperatures were within range of typical surface temperatures during cooling design conditions with solar load on window surfaces and direct solar radiation on room surfaces. The electric powers per one heated dummy were 47 W (160 Btu/h) and 84 W (287 Btu/h), which were quite near sensible heat load of a real occupant. The heat load division uniformly on all room surfaces and on numerous heated dummies differed the test setups from the real office room cases.

ACCEPTED MANUSCRIPT

ACCEPTED MANUSCRIPT

Results

Effect of air distribution

The cooling power of the CRPs increased with the studied air distribution methods. The increase was from 8.6% to 17.1% depending on the air distribution method. Fig. 7 shows the conductance of the radiant panels for the studied cases. The biggest increase to the CRP capacity of about 15.1% was achieved in the radial swirl induction unit case without additional cooling of supply air and 17.1% when additional cooling from the coil of induction unit was used. The increase was approximately 10% in linear and multi-nozzle ceiling diffuser cases.

The calculated centerline velocity, volume flow rate and average temperature of the supply air jet based on manufacturer's data and turbulent air jet theory equations are presented in Table 4. The total pressure levels of the supply air diffusers are also listed for describing the operating conditions of the diffusers. The radial swirl induction unit required the highest total pressure level. All total pressures were within range of typical operating conditions. The supply air jet flow rate just before CRP surface was clearly the biggest in the case of swirl induction unit (approximately 11 times bigger than with 0.9 m (2.95 ft) long linear diffuser and about 4-5 times bigger than with other diffusers). Also the average temperature of supply air jet with radial swirl induction unit at the same location was closest to the room temperature, still differences in the temperatures were not big. The velocity levels varied between 0.29 – 0.95 m/s (0.95 – 3.12 ft/s) levels when the supply air jet reached the CRP surface. The highest increase in cooling power of the CRPs was achieved with radial swirl induction unit, the main reason for this was the high air flow rate of supply air jet just before CRP surface.

ACCEPTED MANUSCRIPT

ACCEPTED MANUSCRIPT

The measured horizontal temperature distribution and vertical temperature distribution in studied cases are shown in Fig. 8 and Fig. 9 respectively. The black ball temperatures were 0.1 - 0.8 ºC (0.18 - 1.44 ºF) higher than air temperature at the two measurement locations because of warm surfaces. The operative temperature calculated from the black ball temperature following the recommendations in standard ISO 7726 (1998) was nearly the same as the black ball temperature at the measured small temperature difference between the air and black ball and assumed velocity less than 0.2 m/s (0.66 ft/s). In all cases with ventilation flow the difference between the black ball temperature and the room air temperature is larger than in the case without ventilation. This is due to the convection power of the supply air jet that has impact mainly on the air temperature. The vertical temperature difference is less than 0.5 ºC (0.9 ºF) in all cases (Fig. 9).

Effect of heat load arrangement

The effect of heat load arrangement on to the performance of CRPs is presented in Fig. 10. The cooling power of the CRPs was decreased by 7% when the heat load was simulated by heated dummies (case 1B) compared to the case when the heat load was conducted through the walls (case 1). In the case 2 with supply air, the cooling power was increased by 10% when comparing it to case 1 without supply air, but this disappeared when comparing case 2B, with dummy heat loads and supply air, to the case 1. Still when comparing case 2B with case 1B (in both cases dummies were used as heat source) there is a 5% increase because of the supply air flushing the CRPs. In the case 2C with uneven heat load distribution (dummies located on one

ACCEPTED MANUSCRIPT

ACCEPTED MANUSCRIPT

side of the room) the increase in the cooling power of the CRPs disappears. This is caused by the colliding local convection flow from dummies with the ventilation flow that can be seen in the smoke visualization shown in Fig. 6D.

The measured horizontal and vertical temperature distribution in the studied cases are shown in Fig. 11 and Fig. 12 respectively. The room air temperature raised over 26 ºC (78.8 ºF) in case 1B because of a bit overestimated electric power of the heated dummies defined from the product data of CRPs and lower cooling power of CRPs with heated dummies. The results in Fig. 11 show that the difference between black ball temperature and air temperature was less than 0.5 ºC (0.9 ºF). The largest difference of air temperature in horizontal and vertical direction was measured in the case 2C where the convection flow of the heated dummies positioned to one side of the test room caused higher temperature readings locally (Fig. 12). Otherwise the vertical and horizontal temperature difference is less than 0.5 ºC (0.9 ºF) in all cases.

Discussion

CRPs were located near the long side wall in order to increase the distance to the supply air diffuser. In this way the cool supply air has time to induce the warm room air and to increase its volume flow rate flushing the CRPs and temperature above the surface temperature of the CRPs. This would enhance the heat exchange between the panels and the flushing air. Another aspect to be considered is that the locations of CRPs near the wall, slightly decreased the velocity of the supply air jet flushing the panel surfaces when it is turning the corner. The set-up used in the present study may be considered to describe the “average” situation in practice.

ACCEPTED MANUSCRIPT

ACCEPTED MANUSCRIPT

The comparison of the cooling power of CRPs was based on the comparion of conductances in the measured cases. This was important because the measured test conditions varied a little due to too high dummy heat load comparing to the actual cooling capacity of the CRPs. The cooling capacity used to define the dummy heat load was based on the manufacturer's product data that was not detailed enough for this type of installation at the time when the measurements were performed. For example the room temperature in the case without supply air and with dummy heat loads (case 1B) was higher than in the other cases (e.g. in case 1B it was 27.8 °C [82.0 ºF] and in case 1, without supply air and with heat loads conducted through walls, it was 26.0 °C [78.8 ºF]). That effected most the case without the cooling power of the supply air. In the cases with dummy heat loads and supply air, the dummy heat load was increased with the average cooling capacity of supply air. The room temperature was closer to 26 °C (78.8 ºF) in the case with symmetrical dummy heat loads (26.4 °C [79.5 ºF] in case 3B) and with uneven dummy heat loads (26.6 °C [79.9 ºF] in case 3C). Still when the conductances were calculated, the cooling performance of the CRP could be compared in different cases. At that time when the comparison was done, the exponent based on product measurements for calculation of the conductance in the suspended ceiling installation was available in the manufacturer's product data (Zehnder Carboline. 2010), which increased the confidence of the comparison. This was assumed to be constant in different cases. In more detailed measurements of each measured case, it could vary a bit. Still the measured conditions were so close to each other, that this was considered to be valid assumption.

ACCEPTED MANUSCRIPT

ACCEPTED MANUSCRIPT

The use of the CRPs with swirl induction unit was quite optimal because the supply air jet from the induction unit was mixture of supply air and induced room air and thus is warmer. Also the volume flow rate of the supply air jet was significantly higher than with other supply air diffusers. In this arrangement the CRPs could also be located nearer the supply air unit and this could increase the cooling perfromance of CRP even more. When cooling from the coil of the induction unit was introduced (case 5), the effect of the suppy air distiribution on the cooling power of CRPs was larger (17.1 %) than without the cooling of the coil (case 4, 15.1 %). That was unexpected, because the heat transfer should be worse when the supply air jet was cooler. The reason for this could be the measurement uncertainty and very small temperature difference of supply air jets in both cases. The effect of the mixing air distribution on the cooling performance of CRP was not very significant with other supply diffuser types. The effect with the multi-nozzle diffuser was almost 10 % with wall heat loads (cases 1 and 3), but it was reduced to about 5 % in the cases with dummy heat loads (cases 1B and 3B). In the real buildings, heat loads are typically a mixture of these types, wall heat loads from wall and window surfaces of the façade, and dummy heat loads from occupants and equipment. This means that the effect of supply air distribution on to cooling performance is somewhere within this range. Based on this research when designing the CRP system, the cooling power of CRPs could be increased safely by 5% in the areas where mixing ventilation supply air jets are flushing the CRP surfaces. This recommendation is based on the cooling powers of CRPs used in the design based on standardized cooling power measurement according EN-14240 (2004) where uniform dummy heat loads are used. This confirms the increase of 6% in the case with radial air distribution and uneven wall and dummy heat loads reported in previous research (Diaz et al.

ACCEPTED MANUSCRIPT

ACCEPTED MANUSCRIPT

2010). The short linear supply air diffuser increased the cooling capacity of CRP by 12% (case 2B), a bit more than the increase by the multi-nozzle diffuser with wall heat loads (case 3). This was most probably caused by the efficient circulation of the room air flushing the radiant panel somehow better than the long linear diffuser, which increased the cooling capacity of about 9% (case 2). That was more substantial than the induction of the room air into the supply air jet, which was the smallest in the case with the short linear diffuser based on the calculation with turbulent jet theory (Table 2). This could be further analysed with CFD simulation.

The case with dummies used as heat load (case 1B) gave a slightly smaller cooling power (7%) than the case with heat load conducted through walls (case 1). Similar setting was studied also earlier with hybrid CRP system and without supply air (Niu et al. 2014) and a bit higher (13%) cooling power with wall heat loads was reported. This same effect can be seen more clearly in the cases with supply air from multi-nozzle diffuser and with wall heat loads (case 3) or with dummy heat loads (case 3B) (11% higher cooling power with wall heat loads). This confirms similar findings reported by Niu et al. (2014) also in the presence of air distribution flushing the surface of CRPs. Niu et al. (2014) reported that the proportion of radiant heat transfer from the heat sources is smaller in the cases with dummy heat loads and affects onto the cooling capacity of CRP system.

In the case with supply air and with uneven dummy heat loads (case 3C) where heated dummies were located only on one side of the room, the generated thermal plumes interact with the ventilation flow resulting in its discharge towards opposite end of the room. For that reason

ACCEPTED MANUSCRIPT

ACCEPTED MANUSCRIPT

the supplied ventilation air does not flush the CRP as efficiently as in the case with symmetrical heat loads. The effect of the heat load arrangement on the cooling power of the CRPs is biggest when the thermal plumes generated by the heat sources (uneven dummy heat loads in the case 3C) affect significantly the distribution of the supply air jet used to enhance the cooling output of the CRP. This can be seen when comparing the cooling power of the case 3 with symmetric wall heat loads to the case 3C with uneven dummy heat loads, both with supply air distribution, where the cooling power was reduced by 16%.

The difference between the air temperature and the operative temperature in the test room was very small in all cases and operative temperature was even bigger than air temperature. As already discussed this was result of the covective cooling of supply air impacting mainly on the air temperature. This was similar as the findings reported in the earlier research (Mustakallio et. al 2016). In the cases without supply distribution, the black ball temperature was a bit higher than in the cases without air distribution especially in the cases with wall heat loads. When dummy heat loads were used this was not so clear.

Conclusions

- The mixing air distribution generated by linear slot diffuser, radial multi-nozzle diffuser and radial swirl induction unit was increasing the cooling power of CRP system from 5% to 17%.

ACCEPTED MANUSCRIPT

ACCEPTED MANUSCRIPT

- The biggest increase in the cooling power was achieved with the high volume supply air jet with temperature near the room air temperature, which was supplied by the swirl induction unit.
- The heat load arrangement in room effected the performance of CRPs both with and without air distribution. The most optimal arrangement for the cooling performance of CRP was uniform wall heat load condition, dummy heat loads load decreased the cooling performance from 7 to 11%. The most significant effect of the heat load arrangement occurs when heat loads are located unevenly and their convection flow turns or weakens the supply air jet flushing the radiant panels.
- In the design of CRP system, the cooling power of CRPs could be increased by 5% in the areas where mixing ventilation supply air jets are flushing the CRP surfaces.
- The difference between the air temperature and the operative temperature in the test room was small.

Acknowledgement

The authors wish to thank Mr. Risto Paavilainen for his participation in the measurement work.

Funding

The study is supported by Technology Agency of Finland (TEKES).

ACCEPTED MANUSCRIPT

ACCEPTED MANUSCRIPT

References

Andrés-Chicote, M., A. Tejero-González, E. Velasco-Gómez, and F.J. Rey-Martínez. 2012. Experimental study on the cooling capacity of a radiant cooled ceiling system. Energy and Buildings 54:207–214.

Ardehali, M.M., N.G. Panah, and T.F. Smith. 2004. Proof of concept modeling of energy transfer mechanisms for radiant conditioning panels. Energy Conversion and Management 45:2005–2017.

Babiak, J., B.W. Olesen, and D. Petras. 2007. Low temperature heating and high temperature cooling, REHVA Guidebook no 7, Finland.

Causone, F., S.P. Corgnati, M. Filippi, and B.W. Olesen. 2009. Experimental evaluation of heat transfer coefficients between radiant ceiling and room. Energy and Buildings 41:622–628.

Diaz, N.F. 2011. Experimental study of hydronic panels system and its environment. Energy Conversion and Management 52:770–780.

Diaz, N.F., J. Lebrun, and P. André. 2010. Experimental study and modeling of cooling ceiling systemsusing steady-state analysis. International Journal of Refrigeration 33:793–805.

EN 14240:2004 Ventilation for Buildings. Chilled ceilings. Testing and rating, European committee for standardization, B-1050 Brussels, Belgium

EN 14518:2005 Ventilation for Buildings. Chilled beams. Testing and rating of passive chilled beams, European committee for standardization, B-1050 Brussels, Belgium

EN 15116:2008 Ventilation in Buildings. Chilled beams. Testing and rating of active chilled beams, European committee for standardization, B-1050 Brussels, Belgium

ACCEPTED MANUSCRIPT

ACCEPTED MANUSCRIPT

EN 15251: 2007 Indoor Environmental Input Parameters for Design and Assessment of Energy Performance of Buildings Addressing Indoor Air Quality, Thermal Environment, Lighting and Acoustics. European Committee for Standardization, B-1050 Brussels, Belgium.

European Commission. Energy Efficiency in the European Union. Available at: https://ec.europa.eu/energy/en/topics/energy-efficiency

European Commission. EPBD Recast: Directive 2010/31/EU of the European Parliament and of the Council of 19 May 2010 on the Energy Performance of Buildings (recast). Available at: http://eurlex.europa.eu/LexUriServ/LexUriServ.do?uri=OJ:L:2010:153:0013:0035:EN:PDF

Fonseca, N. 2011. Experimental study of thermal condition in a room with hydronic cooling radiant surfaces. International Journal of Refrigeration 34:686–695.

Fonseca, N., C. Cuevas, and V. Lemort. 2010. Radiant ceiling systems coupled to its environment part 1: Experimental analysis. Applied Thermal Engineering 30:2187-2195.

Hagström, K., K. Siren, and A.M. Zhivov. 1999. Calculation Methods for Air Supply Design in Industrial Facilities – Litterature review. Report B60. Helsinki University of Technology. Laboratory of Heating, Ventilating and Air-Conditioning. Espoo, Finland. 54, 57.

Halton HIT Design product selection tool. 2015. Halton Oy. Finland.

ISO 7726:1998 Ergonomics of the thermal environment- Instruments for measuring physical quantities, International Organization of Standardization ISO, November 2008, Geneve, Switzerland, pp 16-17, 49-50

Jeong, J.-W., and S.A. Mumma. 2003. Ceiling radiant cooling panel capacity enhanced by mixed convection in mechanically ventilated spaces. Applied Thermal Engineering 23:2293–2306.

ACCEPTED MANUSCRIPT

ACCEPTED MANUSCRIPT

Jeong, J.-W., and S.A. Mumma. 2007. Practical cooling capacity estimation model for a suspended metal ceiling radiant cooling panel. Building and Environment 42:3176–3185.

Jeong, J.-W., and S.A. Mumma. 2004. Simplified cooling capacity estimation model for top insulated metal ceiling radiant cooling panels. Applied Thermal Engineering 24:2055–2072.

Kurnitski, J. et al. 2013. REHVA nZEB technical definition and system boundaries for nearly zero energy buildings. REHVA Technical Report 4.

Mustakallio, P., Z. Bolashikov, K. Kostov, A. Melikov, and R. Kosonen. 2016. Thermal environment in simulated offices with convective and radiant cooling systems under cooling (summer) mode of operation. Building and Environment 100:82-91.

Müller, D., C. Kandzia, R. Kosonen, A. Melikov, and P. Nielsen. 2013. Mixing ventilation: Guide on mixing air distribution design. REHVA Guidebook no 19, Finland.

Niu, X., Z. Tiana, B. Duana, and Z. Wang. 2014. Influences of heat source forms on the cooling capacity of the radiant cooling terminal. Energy and Buildings 72:102–111.

Novoselac, A., J.B. Burley, and J. Srebric. 2006. New convection correlations for cooled ceiling panels in room with mixed and stratified airflow. HVAC&R Research 12(2):279-294.

Rhee, K.-N., and K.W. Kim. 2015. A 50 year review of basic and applied research in radiant heating and cooling systems for the built environment. Building and Environment 91:166-190.

Tian, Z., X. Yin, Y. Ding, and C. Zhang. 2012. Research on the actual cooling performance of ceiling radiant panel. Energy and Buildings 47:636–642.

Woollett, J., J. Rimmer. 2015. Active and Passive Beam Application Design Guide, REHVA-ASHRAE Guidebook no 21, USA.

ACCEPTED MANUSCRIPT

ACCEPTED MANUSCRIPT

Yuan, Y.-L., X. Zhoua, and X. Zhanga. 2015. Experimental Study of Heat Performance on Ceiling Radiant Cooling Panel. Procedia Engineering 121:2176 – 2183.

Zhang, L., X.-H. Liu, Y. Jiang. 2013. Experimental evaluation of a suspended metal ceiling radiant panel

with inclined fins. Energy and Buildings 62:522–529.

Zehnder Carboline Kattolämmitys- ja –jäähdytysjärjestelmä Suunnittelijan esite/ Tekniset tiedot. 2010. Itula Oy. Finland. p 31.

ACCEPTED MANUSCRIPT

ACCEPTED MANUSCRIPT

Table 1. Measured case parameters and cooling powers in the air distribution study

Case	Room (°C)	Supply air (l/s)	(°C)	(W)	(W/m^2_{floor})	Water in panels (kg/s)	in(°C)	out(°C)	(W)	(W/m^2_{floor})	Total cooling (W)	(W/m^2_{floor})
1 No supply air	26.0	0.0		0	0.0	0.043	15.0	17.0	-353	-25.0	-353	-25.0
2 3m Linear air supply	26.1	25.8	15.9	-306	-21.7	0.043	15.0	17.2	-389	-27.6	-695	-49.3
2B 0.9m Linear air supply	25.9	25.0	15.6	-307	-21.8	0.043	15.0	17.2	-386	-27.4	-693	-49.1
3 Radial multi-nozzle	26.1	25.0	15.9	-306	-21.7	0.043	15.0	17.2	-385	-27.3	-691	-49.0
4 Swirl without cooling	25.9	25.0	15.9	-300	-21.3	0.042	15.0	17.3	-401	-28.4	-701	-49.7
5 Swirl with cooling	25.9	25.0	16.2	-292	-20.7	0.045	15.0	17.2	-406	-28.8	-941	-66.8 [1]
Case	(°F)	(cfm)	(°F)	(Btu/h)	($Btu/h/ft^2_{floor}$)	(lb/s)	in(°F)	out(°F)	(Btu/h)	($Btu/h/ft^2_{floor}$)	(Btu/h)	($Btu/h/ft^2_{floor}$)
1 No supply air	78.7	0.0		0	0.00	0.094	59.1	62.6	-1203	-7.93	-1203	-7.9
2 3m Linear air supply	79.0	54.6	60.7	-1043	-6.87	0.094	59.1	63.0	-1327	-8.74	-2370	-15.6
2B 0.9m Linear air supply	78.5	53.1	60.1	-1047	-6.90	0.094	59.0	62.9	-1318	-8.68	-2365	-15.6
3 Radial multi-nozzle	79.0	53.0	60.7	-1043	-6.87	0.094	59.1	62.9	-1315	-8.67	-2359	-15.5
4 Swirl without cooling	78.7	53.0	60.7	-1023	-6.74	0.093	59.0	63.1	-1368	-9.01	-2390	-15.7
5 Swirl with cooling	78.6	53.0	61.1	-996	-6.56	0.099	59.0	62.9	-1387	-9.14	-3211	-21.2 [1]

[1] Additional -243 W (-17.2 W/m^2_{floor}) (-829 Btu/h [-5.45 $Btu/h/ft^2_{floor}$]) cooling from swirl beam unit cooling coil with 0.049 kg/s (0.108 lb/s) water at 15/16.2 °C (59/61.2 °F)

ACCEPTED MANUSCRIPT

ACCEPTED MANUSCRIPT

Table 2. Measured case parameters and cooling powers in the heat load arrangement study

Case		Room (°C)	Supply air (l/s)	(°C)	(W)	(W/m^2_{floor})	Water in panels (kg/s)	in(°C)	out(°C)	(W)	(W/m^2_{floor})	Total cooling (W)	(W/m^2_{floor})
1	No supply air, wall heat loads	26.0	0.0		0	0.0	0.043	15.0	17.0	-353	-25.0	-353	-25.0
1B	No supply air, symm. dummy heat	27.8	0.0		0	0.0	0.043	15.0	17.2	-388	-27.5	-388	-27.5
3	Multi-nozzle air supply, wall heat loads	26.1	24.9	15.9	-305	-21.6	0.043	15.0	17.2	-385	-27.3	-690	-48.9
3B	Multi-nozzle air supply, symm. dummy loads	26.4	25.0	15.7	-320	-22.7	0.043	15.0	17.0	-360	-25.6	-681	-48.3
3C	Multi-nozzle air supply, uneven dummy loads	26.6	25.0	15.7	-327	-23.2	0.043	15.0	17.0	-356	-25.2	-683	-48.4
Case		(°F)	(cfm)	(°F)	(Btu/h)	($Btu/h/ft^2_{floor}$)	(lb/s)	in(°F)	out(°F)	(Btu/h)	($Btu/h/ft^2_{floor}$)	(Btu/h)	($Btu/h/ft^2_{floor}$)
1	No supply air,	78.7	0.0		0	0.00	0.094	59.1	62.6	-1203	-7.93	-1203	-7.9
1B	No supply air,	82.0	0.0		0	0.00	0.094	59.0	63.0	-1325	-8.73	-1325	-8.7
3	Multi-nozzle air supply,	79.0	52.8	60.7	-1039	-6.85	0.094	59.1	62.9	-1315	-8.67	-2354	-15.5
3B	Multi-nozzle air supply,	79.5	52.9	60.3	-1093	-7.20	0.095	59.1	62.7	-1229	-8.10	-2322	-15.3
3C	Multi-nozzle air supply,	79.9	52.9	60.3	-1116	-7.36	0.095	59.1	62.6	-1214	-8.00	-2330	-15.4

ACCEPTED MANUSCRIPT

ACCEPTED MANUSCRIPT

Table 3. Measured surface temperatures and electric powers of heated dummies as compensating heat loads

Case		Room (°C)	Surf.average (°C)	Wall 1 (°C)	Wall 2 (°C)	Wall 3 (°C)	Wall 4 (°C)	Floor (°C)	Dummies (W)
1	No supply air	26.0	26.9	26.8	27.1	26.8	27.1	26.8	0
1B	No supply air, symmetric dummy heat loads	27.8	27.2	27.0	27.3	27.3	27.3	27.3	376
2	3m Linear air supply	26.1	28.6	28.3	28.7	28.5	29.1	28.4	0
2B	0.9m Linear air supply	25.9	27.9	27.4	27.9	27.9	28.5	27.7	0
3	Radial multi-nozzle	26.1	28.3	27.9	28.4	28.3	28.9	28.1	0
3B	Multi-nozzle air supply, symm. dummy loads	26.4	26.4	26.2	26.3	26.4	26.6	26.5	672
3C	Multi-nozzle air supply, uneven dummy loads	26.6	26.5	26.3	26.4	26.2	27.0	26.4	672
4	Swirl without cooling	25.9	28.5	28.1	28.9	28.1	28.9	28.4	0
5	Swirl with cooling	25.9	29.1	28.7	29.7	28.9	29.5	29.0	0
Case		(°F)	(°F)	(°F)	(°F)	(°F)	(°F)	(°F)	(Btu/h)
1	No supply air	78.7	80.4	80.3	80.7	80.2	80.9	80.2	0
1B	No supply air, symmetric dummy heat loads	82.0	81.0	80.7	81.1	81.1	81.2	81.2	1283
2	3m Linear air supply	79.0	83.4	82.9	83.6	83.3	84.3	83.1	0
2B	0.9m Linear air supply	78.5	82.2	81.3	82.2	82.3	83.3	81.9	0
3	Radial multi-nozzle	79.0	82.9	82.3	83.0	82.9	84.0	82.5	0
3B	Multi-nozzle air supply, symm. dummy loads	79.5	79.5	79.2	79.4	79.4	79.8	79.7	2293
3C	Multi-nozzle air supply, uneven dummy loads	79.9	79.7	79.4	79.6	79.2	80.6	79.5	2293
4	Swirl without cooling	78.7	83.3	82.6	84.0	82.7	83.9	83.2	0
5	Swirl with cooling	78.6	84.5	83.7	85.4	83.9	85.0	84.2	0

ACCEPTED MANUSCRIPT

ACCEPTED MANUSCRIPT

Table 4. The calculated supply air jet parameters from different supply air diffusers

Case		Supply air jets leaving the unit				Jet characteristic data			Supply air jet just before CRP		
		dp_t (Pa) [1]	$Q_{0,t}$ (l/s) [2]	v_0 (m/s)	t_0 (°C)	H_0 (m)	A_0 (m2)	K_1 (-) [3]	Q_X (l/s)	v_X (m/s)	t_X (°C)
2	3m Linear air supply	5	25	2.1	16	0.002	-	2.8	130	0.29	25.0
2B	0.9m Linear air supply	2	25	1.4	16	0.01	-	2.8	58	0.43	23.8
3	Radial multi-nozzle	12	25	3.2	16	-	0.0079	1.7	180	0.63	25.3
4	Swirl without cooling	76	70	6.4	23.3	-	0.0108	0.9	667	0.95	25.9
5	Swirl with cooling	76	70	6.4	21.1	-	0.0108	0.9	667	0.95	25.7
Case		dp_t (in W.C.) [1]	$Q_{0,t}$ (cfm) [2]	v_0 (ft/s)	t_0 (°F)	H_0 (ft)	A_0 (ft^2)	K_1 (-) [3]	Q_X (ft/s)	v_X (m/s)	t_X (°C)
2	3m Linear air supply	0.02	53.0	6.9	61	0.0066	-	2.8	276	0.94	77.1
2B	0.9m Linear air supply	0.01	53.0	4.6	60	0.0328	-	2.8	123	1.39	74.8
3	Radial multi-nozzle	0.05	53.0	10.5	61	-	0.0850	1.7	382	2.06	77.5
4	Swirl without cooling	0.31	148.3	21.0	73.9	-	0.1163	0.9	1413	3.12	78.5
5	Swirl with cooling	0.31	148.3	21.0	70.0	-	0.1163	0.9	1413	3.12	78.3

[1] Total pressure drop of supply air in the diffuser at studied operating point

[2] Total supply air jet flow rate: for linear jet 12.5 l/s/jet (26.5 cfm/jet) and for swirl induction unit including also induction flow rate

[3] Throw length coefficient includes effect of ceiling attachment, confinement of test room and swirl pattern

ACCEPTED MANUSCRIPT

ACCEPTED MANUSCRIPT

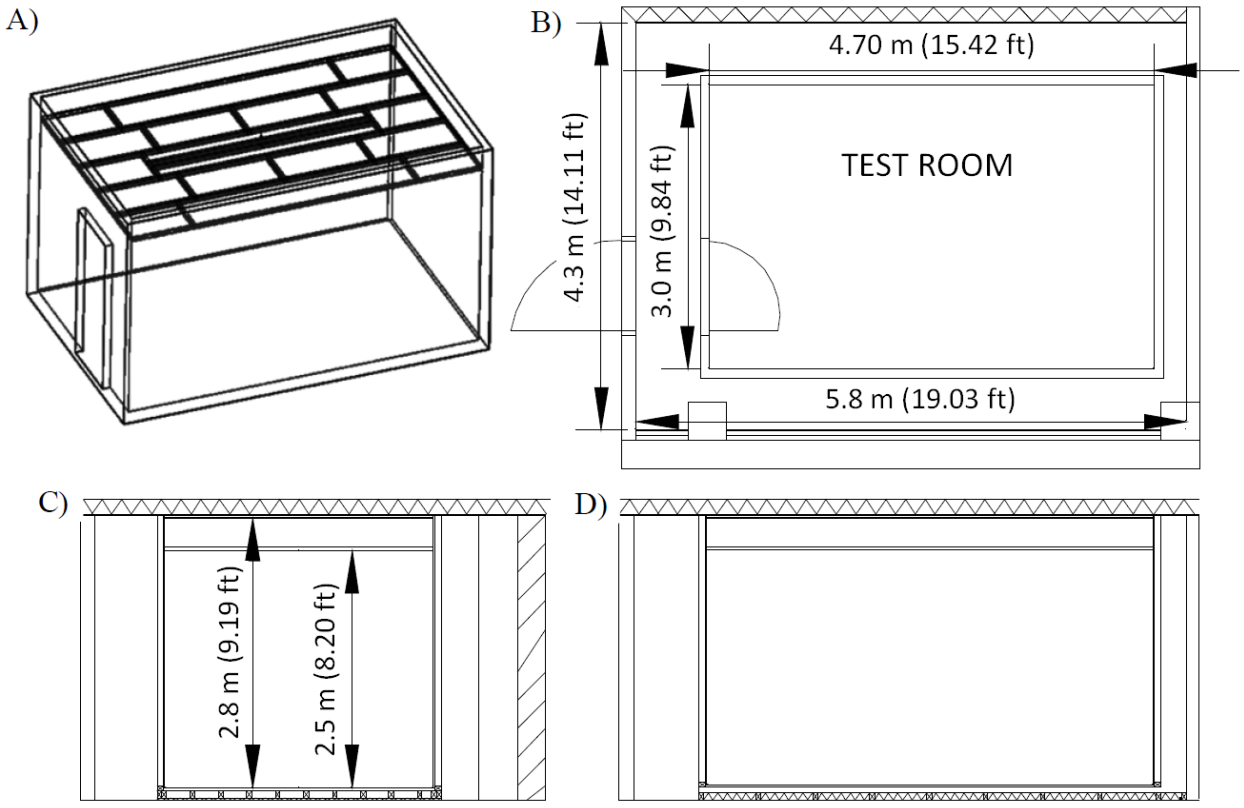

Fig. 1. Construction of the full-scale test room: A) Geometry of the full-scale test room with suspended ceiling shown in case 2, B) top view of the test room and external room with constant temperature, C) side view (widthwise) and D) side view (lengthwise)

ACCEPTED MANUSCRIPT

ACCEPTED MANUSCRIPT

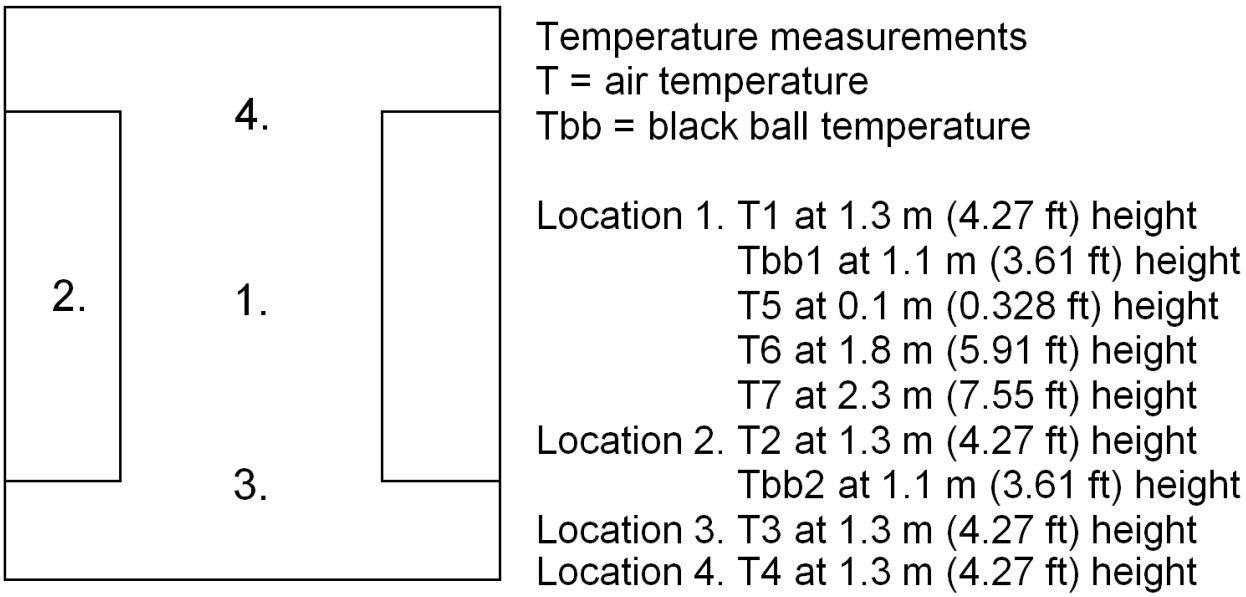

Fig. 2. Top view of the full-scale test room on the left side and locations of the temperature measurement sensors in the test room on the right side

ACCEPTED MANUSCRIPT

ACCEPTED MANUSCRIPT

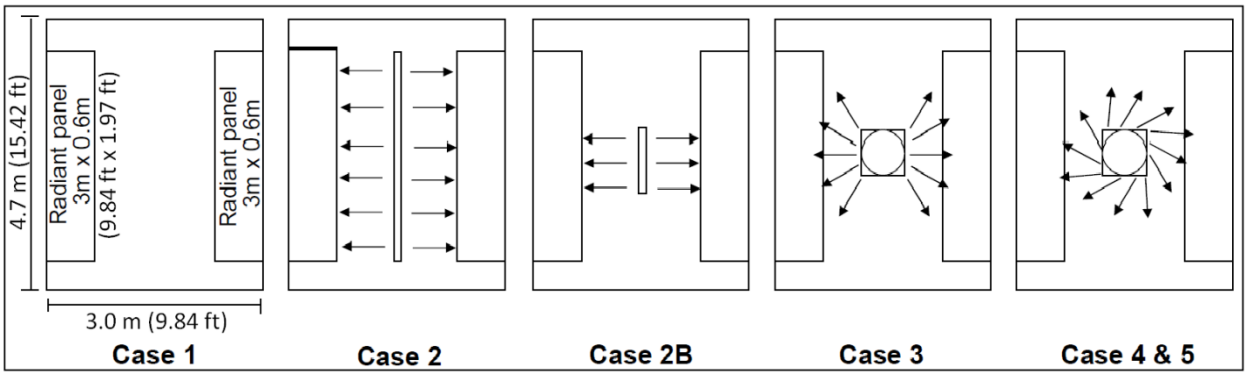

Fig. 3. Top view of the full-scale test room presenting test cases for analysis of the effect of air distribution on the cooling power of CRPs

ACCEPTED MANUSCRIPT

ACCEPTED MANUSCRIPT

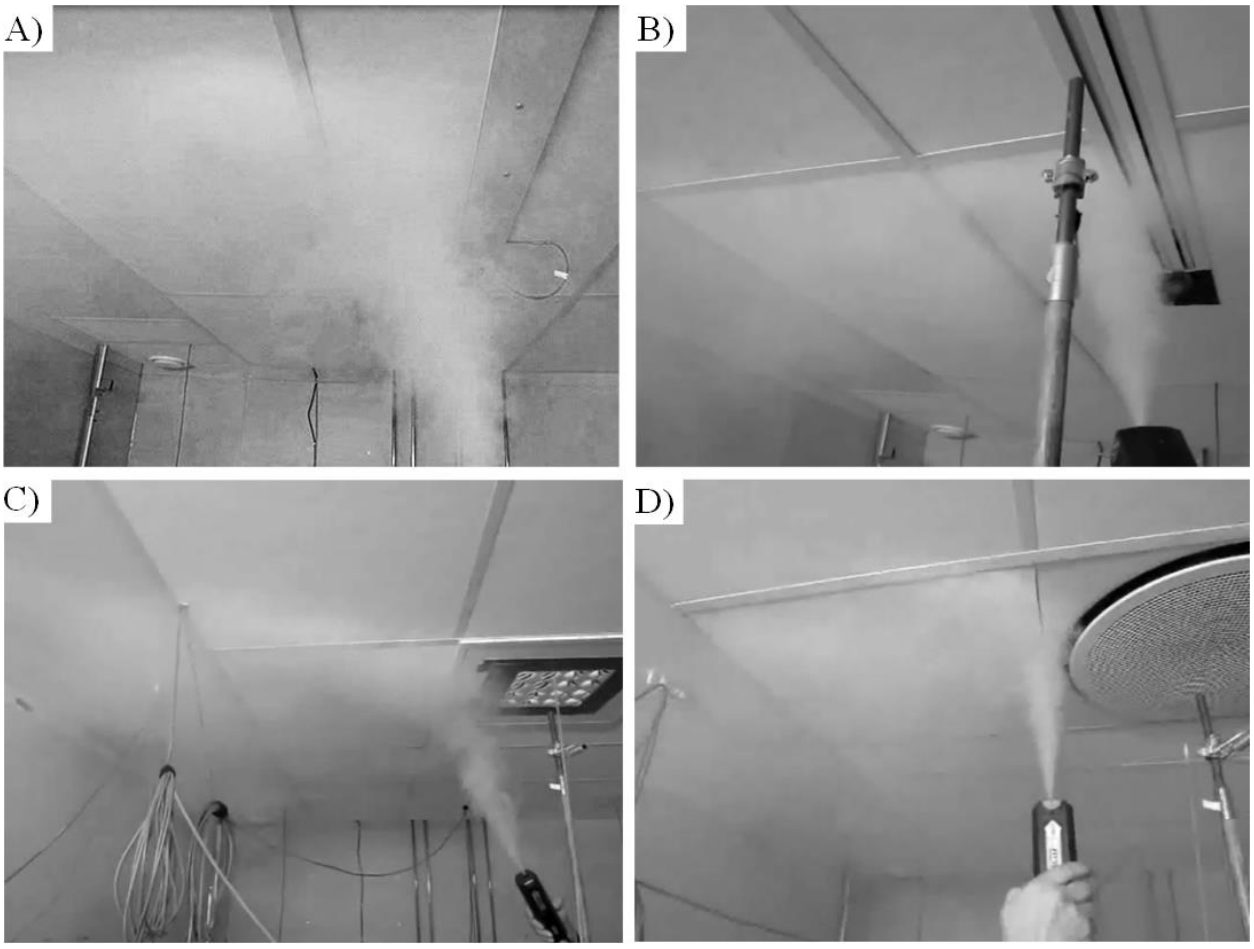

Fig. 4. Smoke visualizations of air supplied from A) the 3 m (case 2) and B) the 0.9 m long linear slot diffuser (case 2B), C) the radial multi-nozzle diffuser (case 3) and D) the radial swirl induction unit (case 4)

ACCEPTED MANUSCRIPT

ACCEPTED MANUSCRIPT

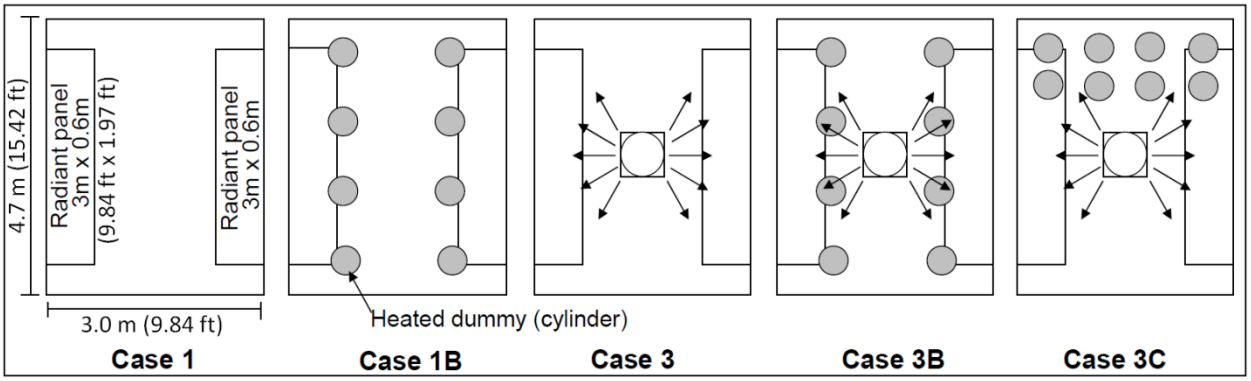

Fig. 5. Top view of the full-scale test room presenting test cases for analysis of the effect of heat load arrangement on the cooling power of CRPs

ACCEPTED MANUSCRIPT

ACCEPTED MANUSCRIPT

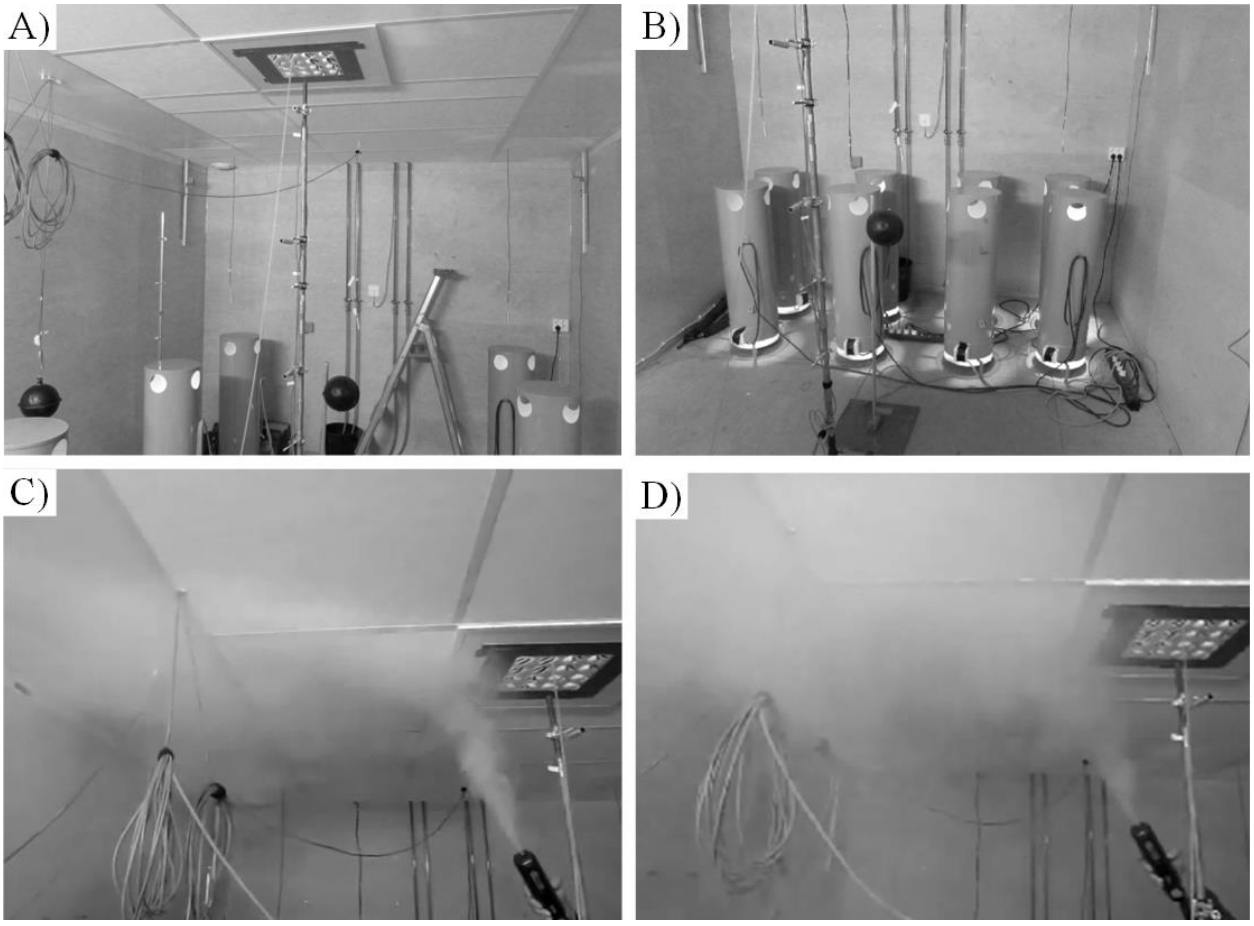

Fig. 6. A) Overall view of the setup with heated dummies positioned symmetrically; B) heated dummies positioned unevenly, i.e. only in one side of the test room, C) supply air jet smoke visualizations in case 1 and D) in case 2C.

ACCEPTED MANUSCRIPT

ACCEPTED MANUSCRIPT

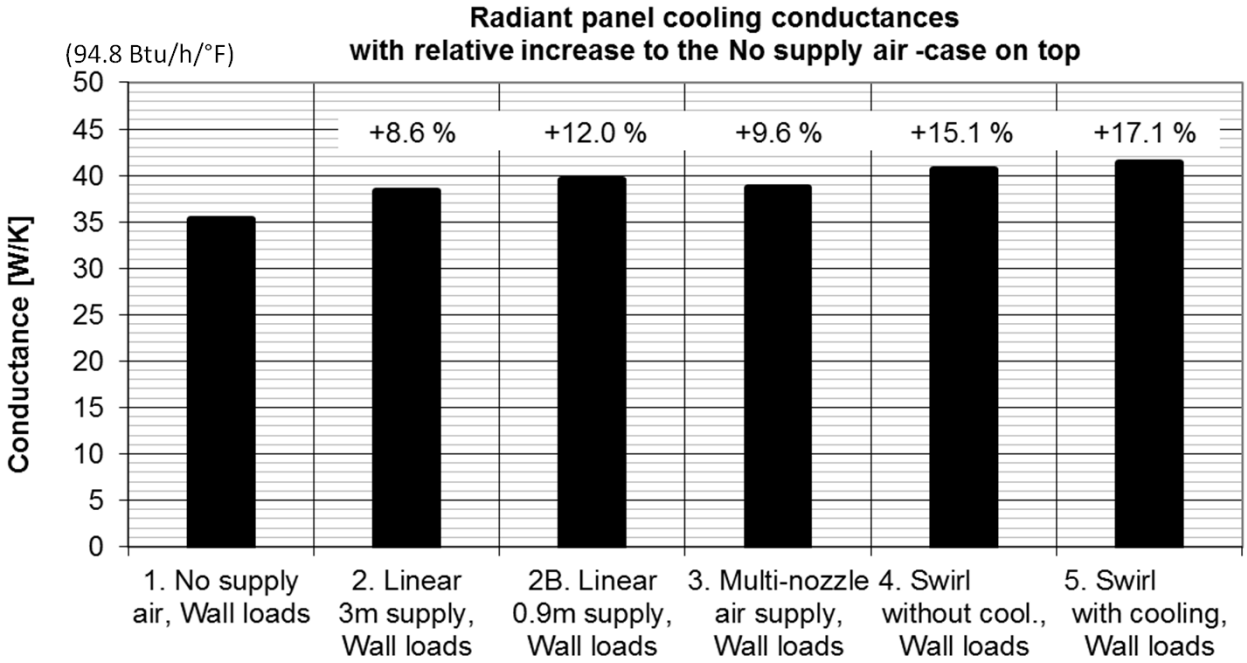

Fig. 7. CRP conductances in cooling mode in studied cases and increment of cooling capacity of panel compared with the case 1 without supply air

ACCEPTED MANUSCRIPT

ACCEPTED MANUSCRIPT

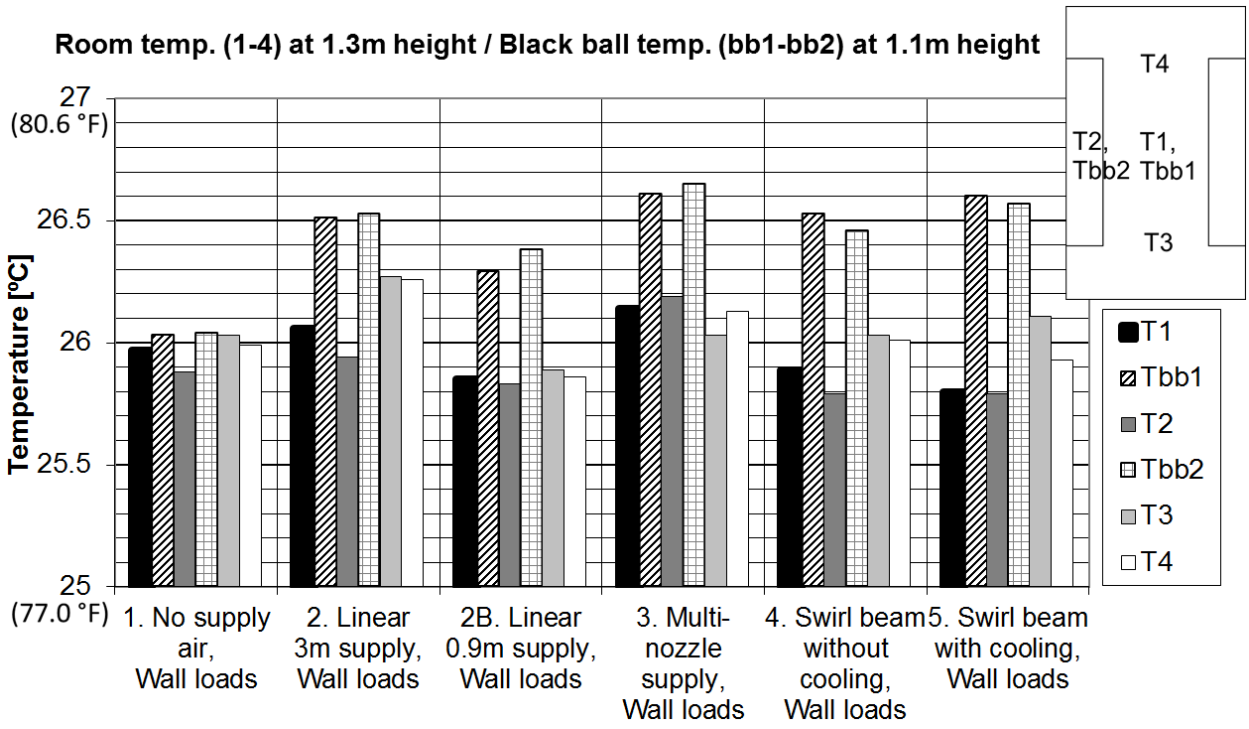

Fig. 8. Room temperatures and black ball temperatures in the occupied zone (locations are specified in Fig. 2)

ACCEPTED MANUSCRIPT

ACCEPTED MANUSCRIPT

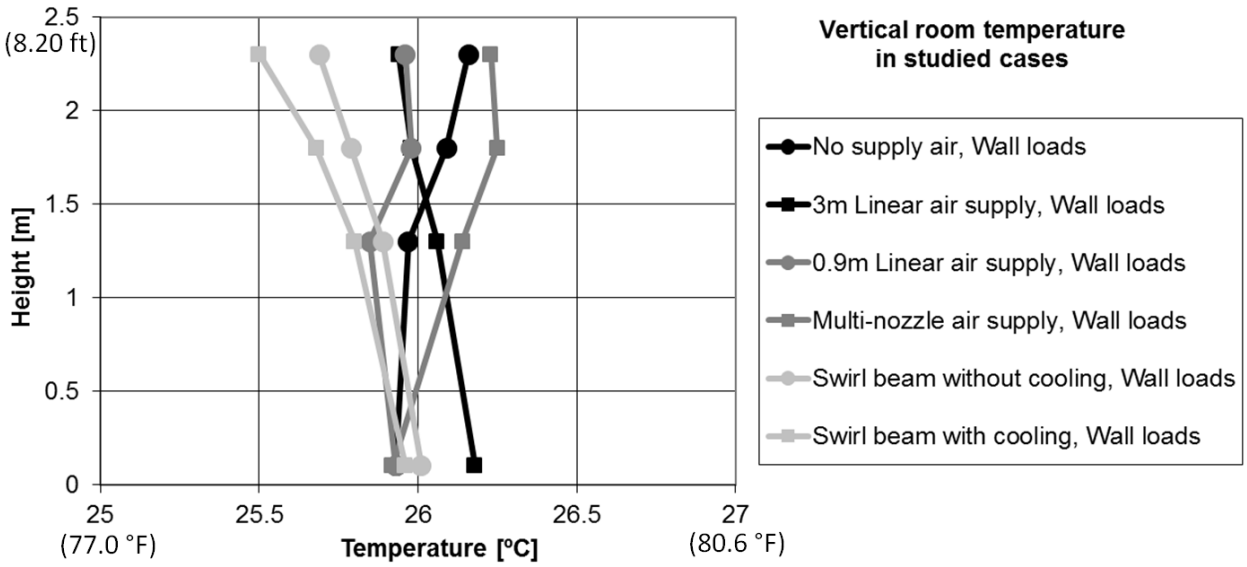

Fig. 9. Vertical temperature distribution measured in the studied cases

ACCEPTED MANUSCRIPT

ACCEPTED MANUSCRIPT

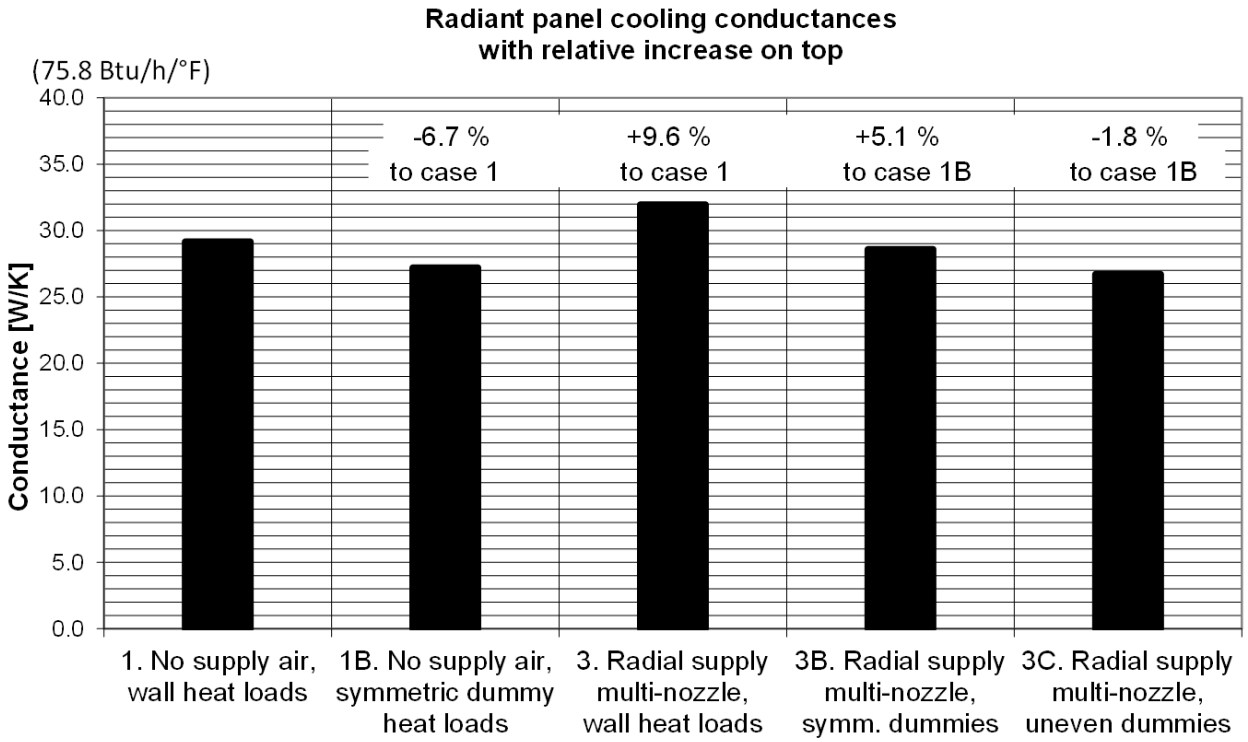

Fig. 10. CRP conductances in cooling mode in studied cases and comparison to the case 1 and 1B without supply air

ACCEPTED MANUSCRIPT

ACCEPTED MANUSCRIPT

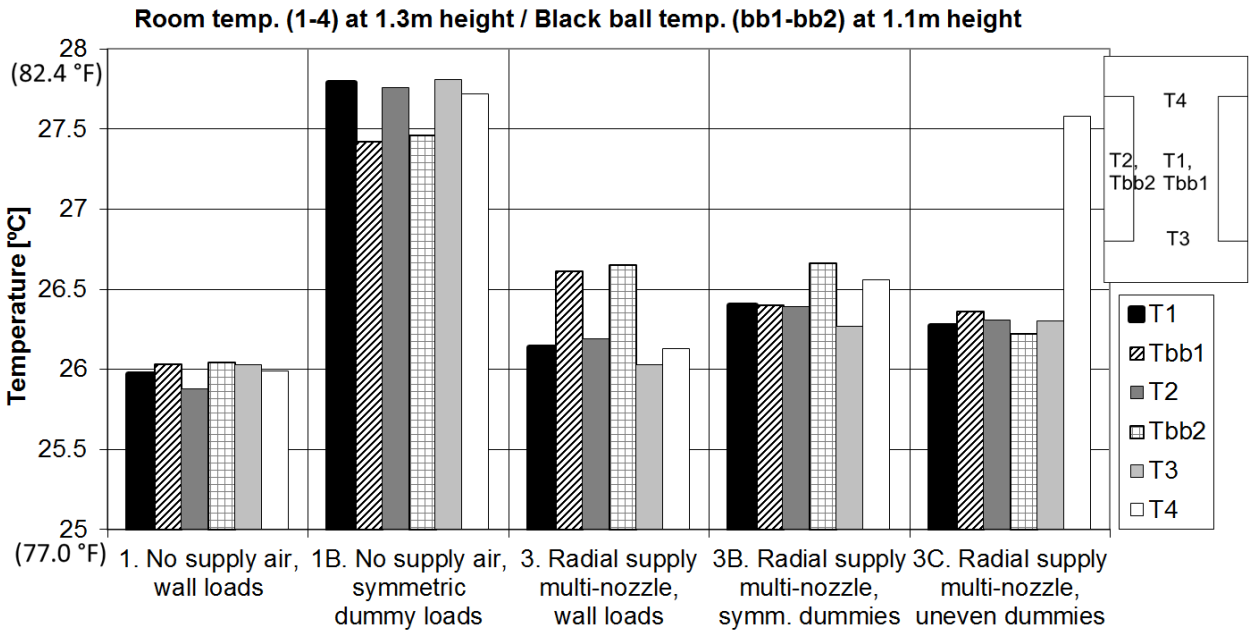

Fig. 11. Room temperatures and black ball temperatures in the occupied zone (locations are specified in Fig. 2)

ACCEPTED MANUSCRIPT

ACCEPTED MANUSCRIPT

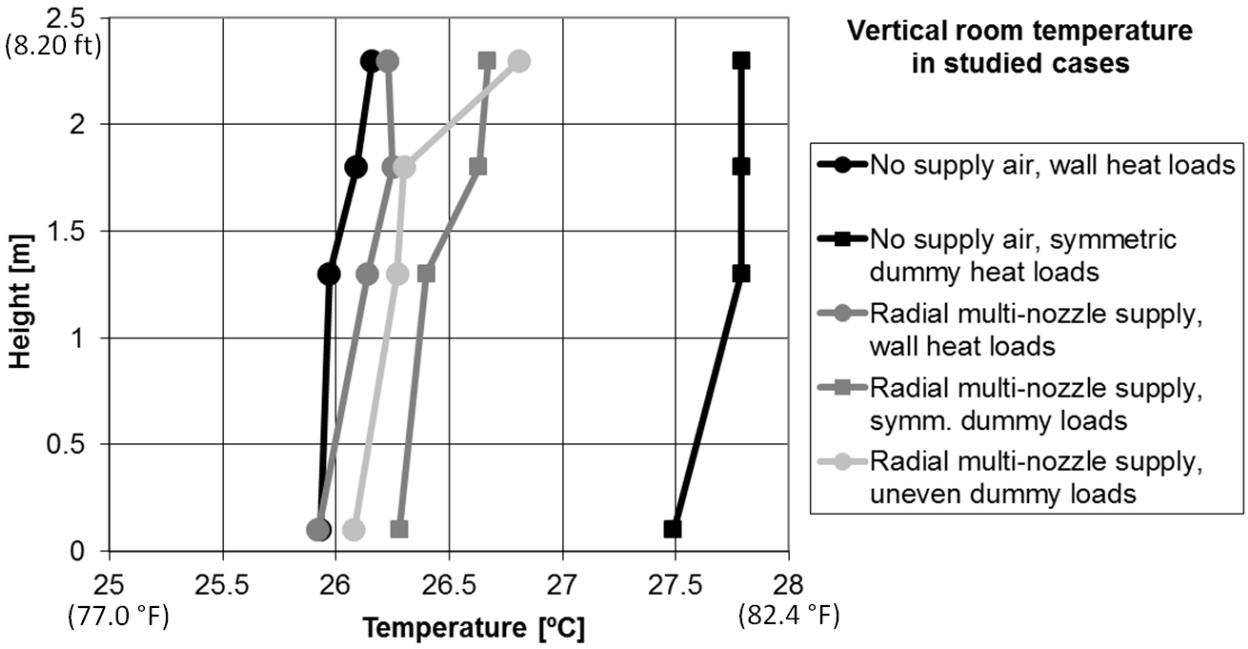

Fig. 12. Vertical temperature distribution measured in the studied cases

ACCEPTED MANUSCRIPT